Localisation and identification of fatigue matrix cracking and delamination in a carbon fibre panel by acoustic emission

Davide Crivelli [a,*], Mario Guagliano [a], Mark Eaton [b], Matthew Pearson [b], Safaa Al-Jumaili [b], Karen Holford [b], Rhys Pullin [b]

[a] Politecnico di Milano, Department of Mechanical Engineering, via La Masa 1, 20156 Milano, Italy
[b] Cardiff School of Engineering, Cardiff University, Queen's Building, The Parade, Cardiff CF24 3AA, Wales, UK

Received 9 April 2014
Received in revised form
6 November 2014
Accepted 30 December 2014
Available online 12 January 2015

1. Introduction

The growing use of composite materials is encouraged by those industrial sectors in search of lightweight materials, which guarantee the same safety levels and reliability as those in traditional metallic structures. A solution is to equip those structures with an on-board sensing technique, capable of detecting damage. This family of techniques goes under the name of Structural Health Monitoring (SHM), comprising all those systems that monitor, either continuously or at specific moments, the health status of a material, giving an indication to the user about damage developing, damage severity and eventually damage location [1].

Such SHM systems, if appropriately designed, will also allow a reduction in the downtime of assets. Planned, inspection-interval based maintenance will no longer be required in favour of an on-demand maintenance programme. Safety critical structures, such as off-shore wind turbines or aircrafts, will receive the most benefit from this approach to monitoring, since their maintenance downtime represents a large part of their operative cost.

Among the SHM techniques being investigated at the moment, Acoustic Emission (AE) is considered to be a good candidate [2]. AE is based on the observation that materials, when undergoing some type of damage, release energy in the form of short, transient elastic waves in the ultrasound band (100 kHz–1000 kHz). These waves propagate in the structure through the material's bulk and surface, and eventually dissipate due to various phenomena. These waves can be recorded by means of appropriate sensors, usually of the piezoelectric type [3].

AE is classified as a passive Non Destructive Technique (NDT): it does not require signals to be emitted (i.e. to introduce energy in the structure) to detect damage. Instead, it waits for signals to be recorded; those signals originate inside the material by some damage or energy release process. This is a major advantage of AE, as it does not require continuous scanning of the structure or the continuous recording of data in search of a potential defect. This is however also a downside, because it does not provide information about a structure when it is not loaded, unlike other NDTs (like radiography or ultrasound). In other words, the source must be active to be detected; unstressed flaws will not generate AE.

* Corresponding author. Tel.: +39 02 2399 8595; fax: +39 02 2399 8202.
E-*mail addresses:* davide.crivelli@polimi.it (D. Crivelli), mario.guagliano@polimi.it (M. Guagliano), eatonm@cardiff.ac.uk (M. Eaton), pearsonmr@cardiff.ac.uk (M. Pearson), al-jumailisk@cardiff.ac.uk (S. Al-Jumaili), holford@cardiff.ac.uk (K. Holford), pullinr@cardiff.ac.uk (R. Pullin).

There are several sources of AE. In metallic structures, AE can arise from crack propagation and plastic deformation [4], as well as from non-detrimental phenomena such as friction and bonding relative movement. Spurious noise sources from parts that are acoustically connected are also a concern. In composite structures, AE sources are associated with the main failure modes of those materials: fibre breakage, matrix cracking, fibre pull-out and delamination [5]. An in-depth analysis of these AE events can lead to source type identification based on waveform characteristics; this is the subject of current extensive research [6]. Especially in composite materials, AE has proved to offer interesting indications to researchers about the development of damage. Static tests, but also fatigue tests [7–9], crack propagation, bond strength tests [10], residual strength tests [11] and many others have benefited from AE monitoring.

For all these applications, the necessity to identify different AE sources emerges. The main concern is to learn how to assess whether and when a specific failure mode occurs in a material; such research is usually aimed at increasing the knowledge regarding failure modes of materials or structures and is directed towards the development of better damage models.

One of the advantages of AE is its ability to localise damage sources by using multiple sensors (three or more for localisation on a plane [3]). Common planar location algorithms usually consider a uniform velocity in the whole plane; then, based on the time of arrival (ToA) of the waveforms, they compute the position by intersection of hyperbolas between sensor pairs. This algorithm is robust for homogeneous materials, provided that the waveforms ToA is computed correctly and the velocity is known with an adequate precision. However, in anisotropic materials, such as Carbon Fibre Reinforced Polymers (CFRP), the wave velocity depends on the orientation of the wavepath with respect to the ply orientation. This makes the ToA technique prone to errors. Moreover, local features (such as material's local inhomogeneities and discontinuities) add uncertainty to the problem. To overcome this issue, a technique called Delta-T was developed [12,13]. Delta-T utilises user-generated maps of ToA differences between sensors, without defining a wave velocity but with the help of a calibration grid. A HSU-Nielsen source [14] is generated at each grid point; subsequently, for each sensor pair, a ToA difference map is computed. The location algorithm then, when receiving a waveform (or, more specifically, the sensor pairs ToA differences) looks up each Delta-T map and identifies the source location. This technique proved to be more accurate than the ToA method in a number of test cases [15].

Commercial AE systems already provide some sort of data compression, by encoding the information contained in each waveform into different parameters, such as peak amplitude, frequency content, duration, energy and some others. Moreover, these parameters are thought to be linked to the kind of damage source that originated the signal. For SHM based on AE, this feature would be helpful because it provides information not only on the event localisation, but also on the activity of specific damage modes.

In composite materials, AE can be generated in a number of ways; the main failure modes include matrix cracking, fibre-matrix debonding, fibre fracture and delaminations. There are differences in the nature of the AE signals due to the source type; this is mainly due to the in-plane or out-of-plane energy content. It is known that matrix cracking and fibre breakage initiate mostly in-plane phenomena and generate extensional waves of higher frequency, while delaminations are dominated by flexural waves of lower frequency [16].

In a delamination, the laminate separates at the interface between two layers, in some cases without indications on the surface (for example, some impacts, although not visible from the impacted surface, may hide large delaminations). Some authors suggest delaminations give rise to high amplitude signals [17], while others point out medium amplitude signals for a $\pm 45^\circ$ laminate [18]; authors generally agree on delamination signals having in general a long duration [19], but tend to include debonding within the same classification.

Matrix cracking generally occurs between fibres at the fibre-matrix interface, or as shear failures between plies. These types of matrix failures usually cause hackles, which are visible on the surface. Results have been found to be dependent on material and testing procedure, with some agreement on defining matrix cracking AE as mid-to-high amplitude and low frequency [20], but some studies report low amplitude [17,18,21] and medium frequency [22] fast decay [23] but also slow decay [24].

Finally during loading, some fibres fail in tension. The expected AE signature is an abrupt energy release mechanisms, with high amplitude and fast rise time [18], as it would happen in a brittle crack phenomenon.

As discussed, early approaches based the classification of damage mechanisms on a single AE parameter, typically peak amplitude or frequency content. When trying to overcome some issues, mainly related to signal attenuation as a function of distance, multiple parameters at once have been considered [21,25]. Due to the high amount of data to be processed and difficulties in identifying patterns with traditional statistical techniques, machine

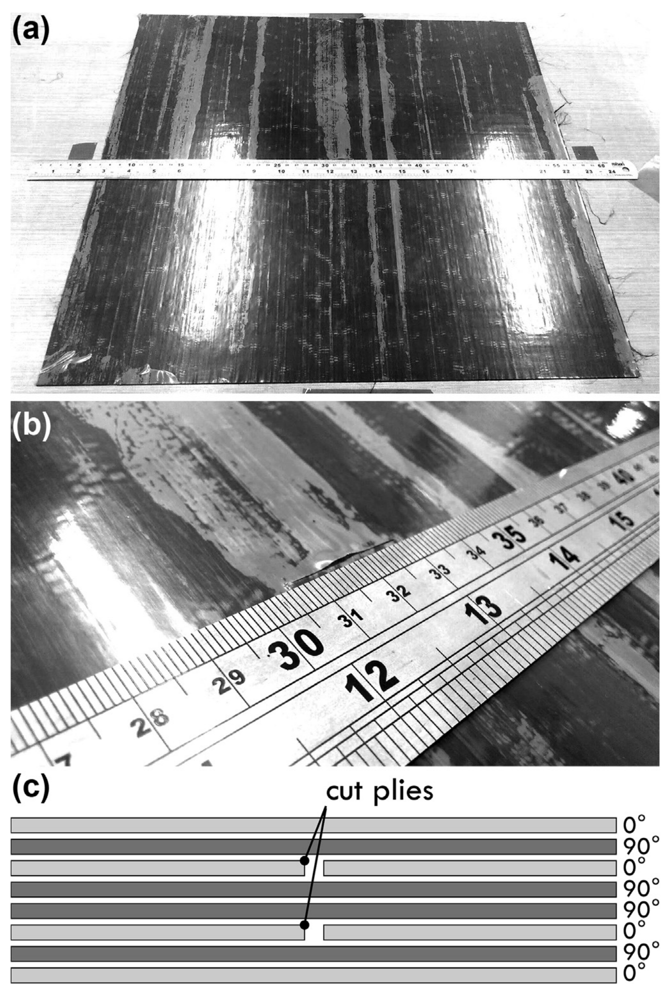

Fig. 1. CFRP panel during layup of the inner plies: entire panel (a), detail of the cut (b) and cut plies schematic (c).

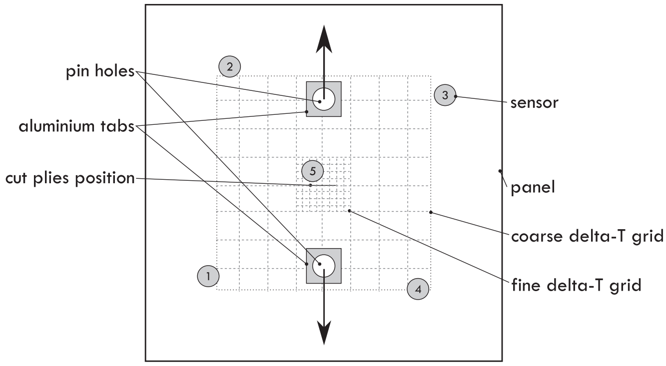

Fig. 2. Artificial crack panel after manufacturing.

learning algorithms, especially Artificial Neural Networks (ANN), have been increasingly used in this field [26–30]. Among these techniques, a previous paper by the authors [31] presented an unsupervised technique for the classification of AE signals, based on the Self Organizing Map (SOM) and the k-means clustering algorithm. The technique, for brevity referred to as *k-SOM*, also employs a number of clustering indexes to determine which is the optimal number of natural classes found in a dataset. In this way, no user input or tuning is required.

The aim of this experimental work is to obtain, analyse and identify AE signals from different damage sources. These sources should be generated in a way that they could be easily isolated from boundary effects (like edge reflections), while at the same time being in a known and distinct location. The positive identification of different damage sources by the *k-SOM* classification technique is key to separate the different contributions of the various AE modes in a real structure; for this reason, it is the intention of this work to provide a further validation of the technique.

2. Experimental plan

2.1. Panel

A 500 mm × 500 mm CFRP panel was manufactured from unidirectional pre-preg T800S carbon fibre (56.6% in volume) in epoxy resin (M21/35%/UD268/T800S, Hexcel Corporation). The final laminate consisted of eight layers, laid up as $[0/90]_{2S}$, giving a total thickness of 2.2 mm; this was in line with the indications of the manufacturer (a 2.1 mm thickness was expected).

To promote matrix cracking in the innermost 0° layers (3rd and 6th) a 25 mm crack was introduced by cutting the fibres with a knife. Particular attention was paid when manufacturing the final lay-up to ensure that the two cracked layers were aligned (Fig. 1). This would ensure matrix cracks are more likely to happen in this area as these plies are no longer supported by longitudinal fibres in the direct loading path.

The panel was then cured as per manufacturer specifications in an autoclave. The panel was subsequently C-scanned to make sure that no macroscopic defects or curing failures were present.

To allow the panel to be loaded in tension, two holes were drilled and reinforced with aluminium square tabs. This helped

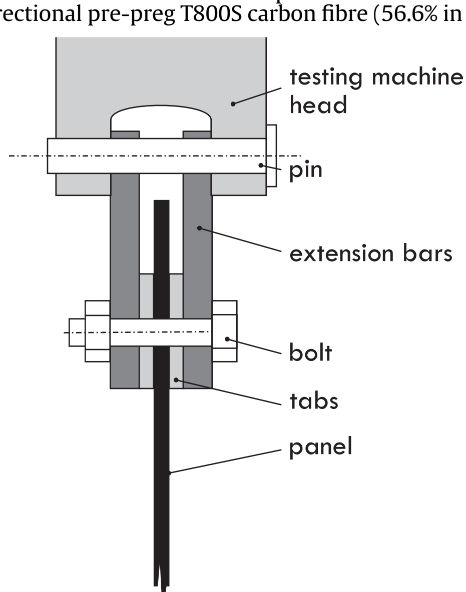

Fig. 3. Panel fitting in the tensile machine.

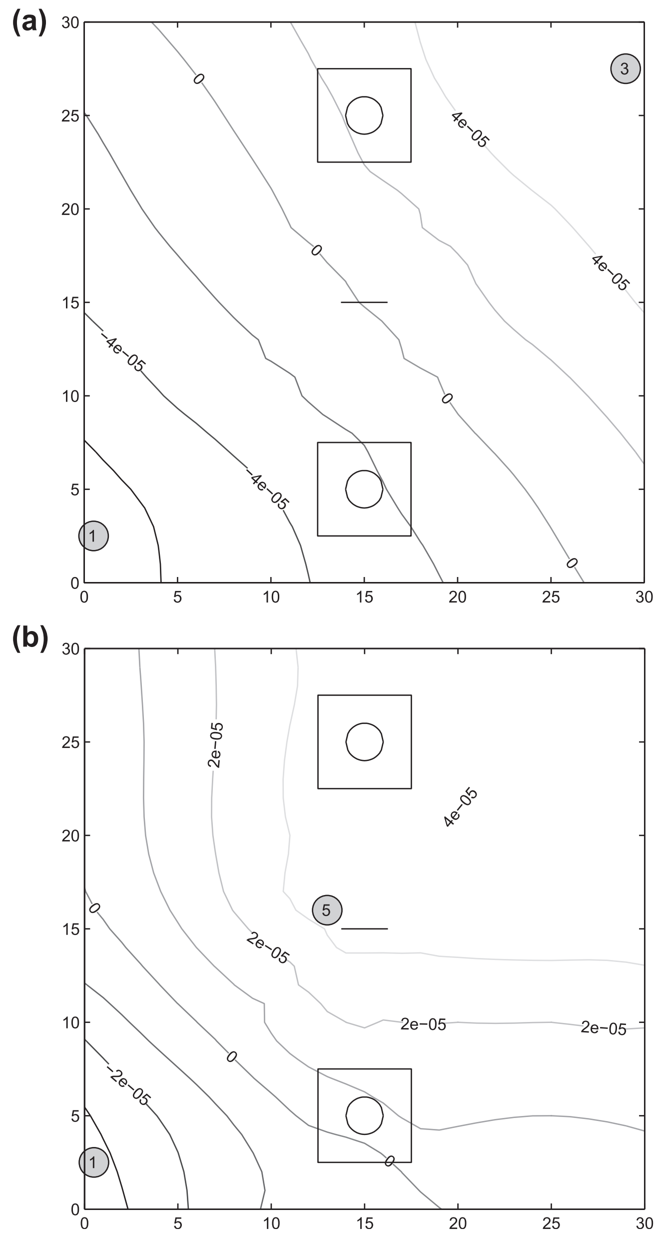

Fig. 4. Examples of Delta-T calibration maps for sensors 1–3 (a) and 1–5 (b).

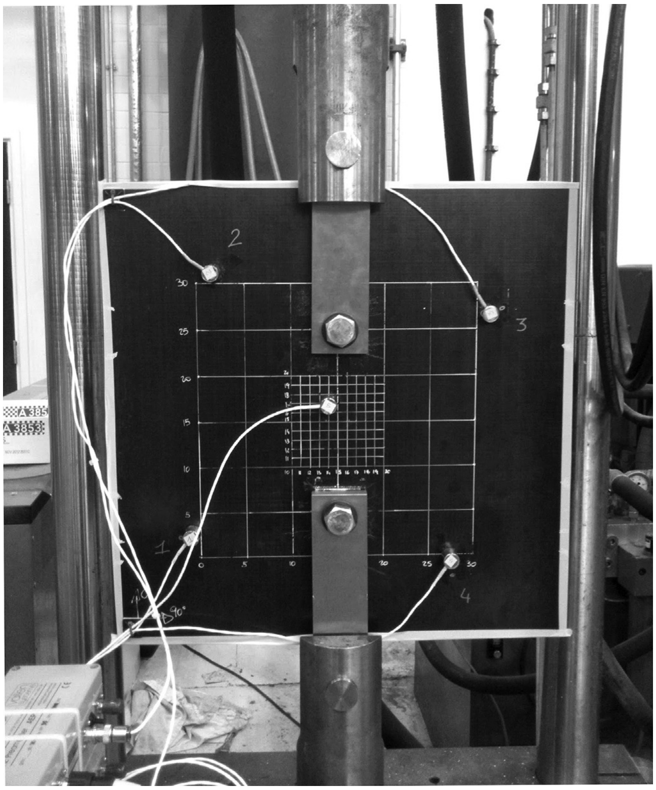

Fig. 5. Panel with sensors and fitted in the testing machine.

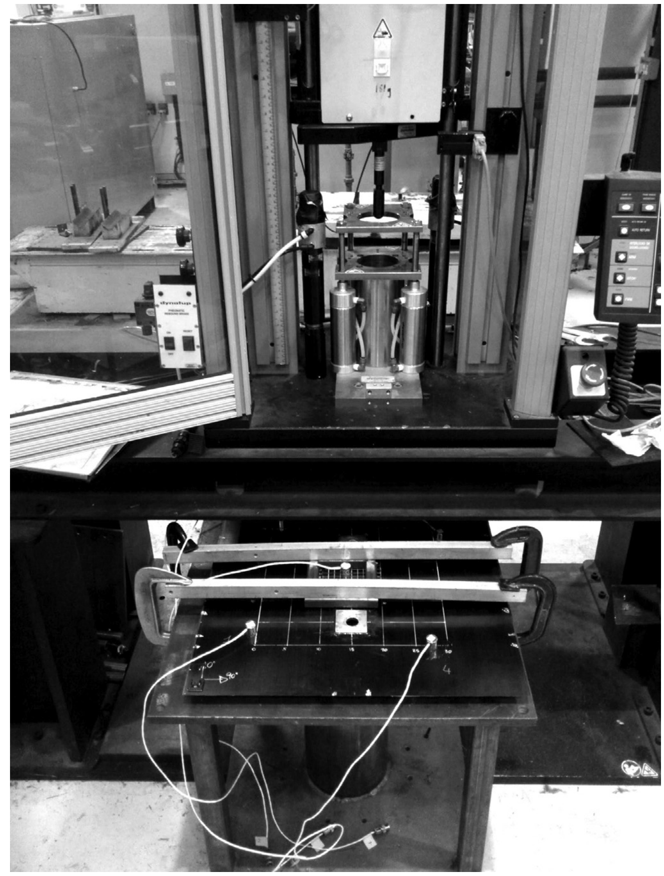

Fig. 6. Impact machine and panel fitting.

avoid damage deriving from the direct contact between the fixture and the panel surface.

The tabs were bonded before cutting the holes with araldite glue; the holes were then drilled through both aluminium and the material. Another C-scan was then performed to compare with the original scan to make sure that it was not damaged during this process. The final panel geometry is shown in Fig. 2.

A schematic drawing of the specimen in the tensile machine is shown in Fig. 3.

2.2. AE setup

For this test, a Vallen AMSY-4 system was used. Physical Acoustics Corporation WD (wideband) sensors were connected to Vallen AEP3 pre-amplifiers, with the gain set to 34 dB. A band-pass filter between 95 kHz and 1000 kHz was used. Sampling frequency for waveforms was set to 5 MHz with a set length of 4096 points, corresponding to a 819.2 μs wavelength. Noise threshold was set to 44.9 dB.

The panel was then prepared for the Delta-T location calibration. A square grid was drawn with two resolutions (Fig. 2): the bigger one, 300 mm × 300 mm wide, featured a 50 mm spacing; in the central region a finer grid was drawn, with a 10 mm spacing and a 100 mm × 100 mm size. The smaller grid is used to get a more accurate location of damage in the cut plies region.

Two examples of the Delta-T maps are shown in Fig. 4 (ten are created in total, one for each sensor pair). It is interesting to observe how the Delta-T technique allows for compensation of the disturbances of wave propagation around the tabs and local anisotropies in the wave velocity due to the material's layup.

2.3. Testing plan

After Delta-T calibration, the panel was fitted into the load test machine. A pin, running through each extension bar hole, connected the panel to the load test machine. The panel was then bolted into the extension bars (Figs. 3 and 5). The bolts were tightened before starting the test, thus using friction to improve the load transfer between the machine and the panel. Particular care was used in making sure that the extension bars were vertical at almost-zero load. The panel fitted in the testing machine can be seen in Fig. 5.

Table 1
Peak load levels for the pre-impact phase.

Batch nr.	Load (kN)	Batch nr.	Load (kN)	Batch nr.	Load (kN)
1	8	9–11	12	19	17
2	8	12–13	13	20–21	18
3–5	9	14–16	14	22	19
6–7	10	17	15	23–25	20
8	11	18	16	26	21

Table 2
Peak load levels for the post-impact phase.

Batch nr.	Load (kN)	Batch nr.	Load (kN)	Batch nr.	Load (kN)	Batch nr.	Load (kN)
1	14	6	20	15	24	21–22	28
2	16	7–8	21	16–17	25	23–24	29
3	18	9–11	22	18	26	25–30	30
4–5	19	12–14	23	19–20	27	31	31

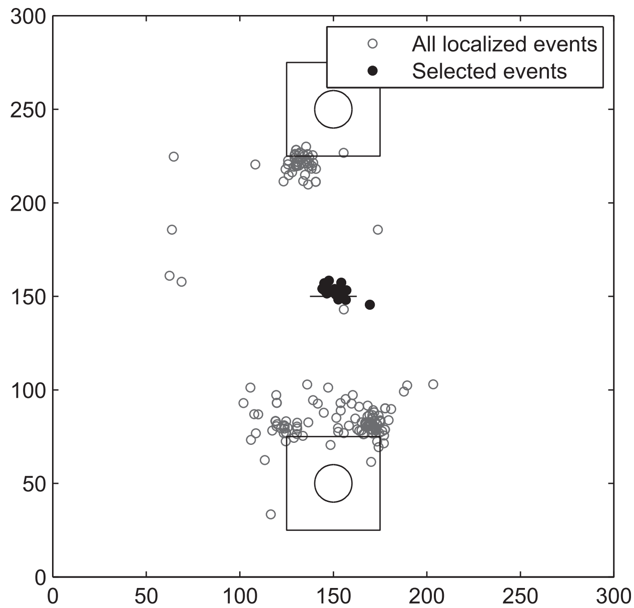

Fig. 7. Location of AE events from the crack propagation test.

The testing plan consisted in running fixed-amplitude batches of 5000 cycles, at 1 Hz; after each batch the panel was removed from the rig and C-scanned, monitoring the eventual damage growth in the panel. The load was increased after each batch if none or little AE was observed, otherwise another run was made at the

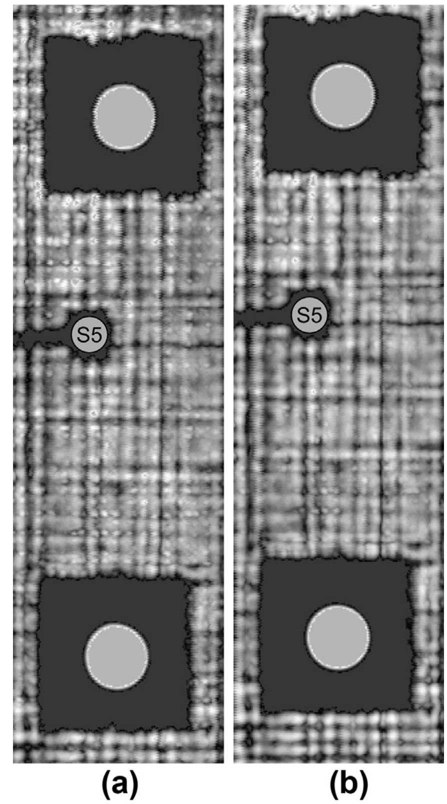

Fig. 9. C-scan images of the panel central region as manufactured (a) and before impact (b), also showing sensor location.

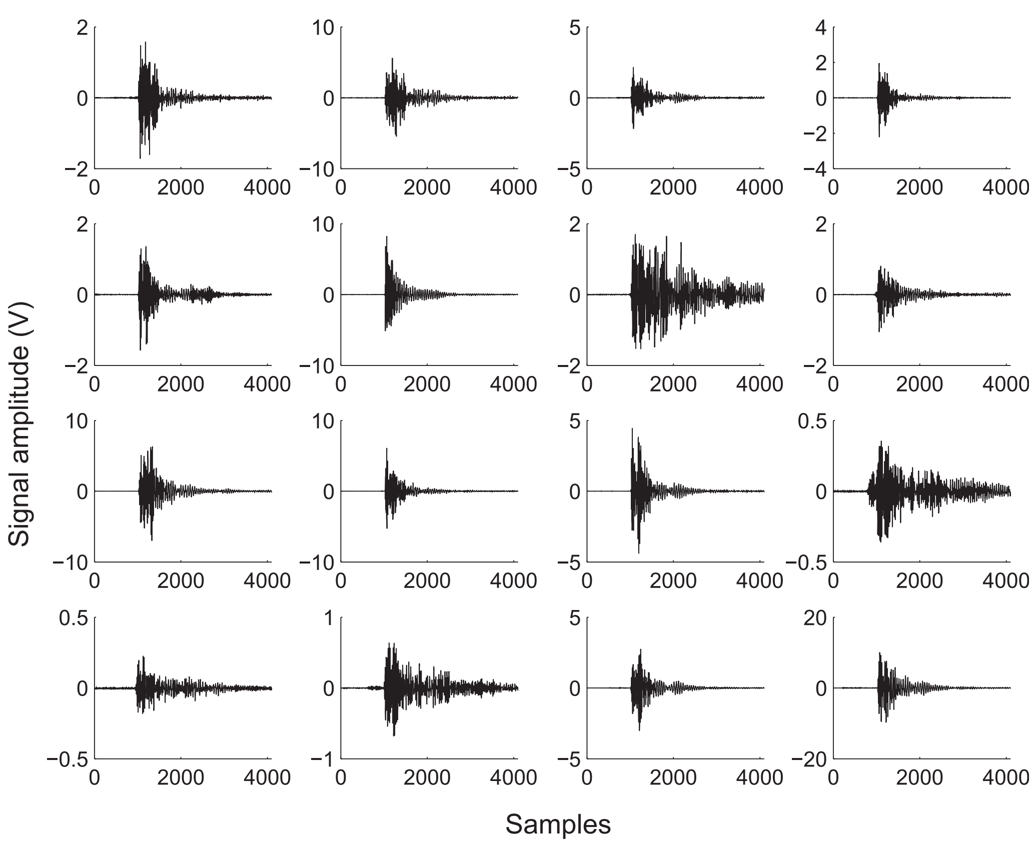

Fig. 8. AE events from crack region.

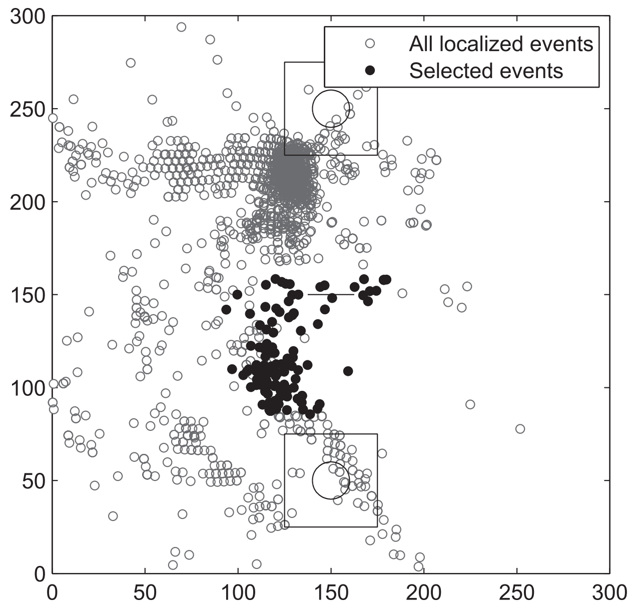

Fig. 10. AE events during the selected after impact batch.

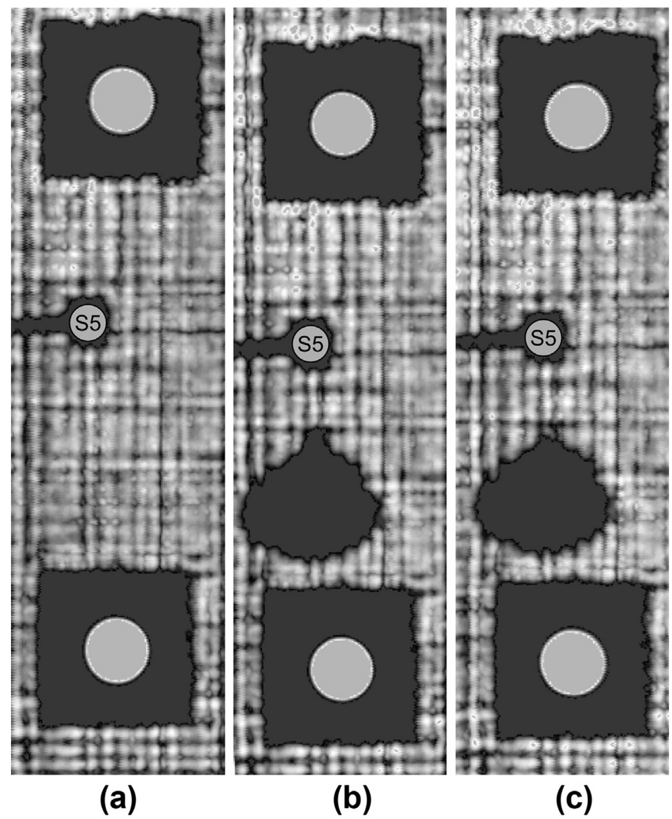

Fig. 12. C-scan images of the panel before impact (a), after impact (b) and end of test (c).

same load level. Tests were run with an R ratio (min load/max load) of 0.1 to avoid compression loads and to obtain a sufficient preload in the fitting. The peak loads are summarised in Table 1.

After a sufficient number of AE signals from the artificial crack area were collected (to allow source characterisation), the panel was then impacted with an Instron Dynatup 9250HV impact

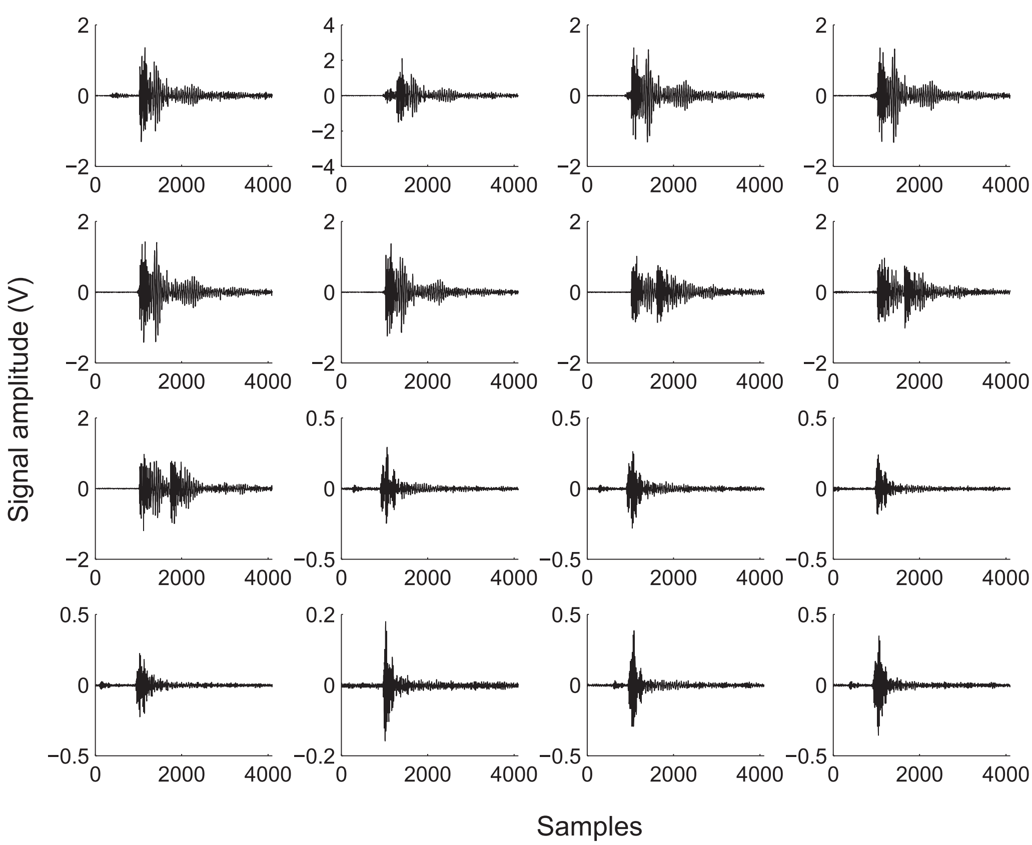

Fig. 11. AE events from delamination region.

machine at an energy of 14J, in a location far from the crack but still within the loading path of the test. The impact machine, with the panel frame fitting, can be seen in Fig. 6.

The purpose of the impact was to generate signals from both the crack and the delamination resulting from the impact. The panel was then tested again as previously, increasing the load and C-scanning after every batch of loading (Table 2).

3. Results

3.1. Pre impact

During the first phase of testing, about 40 AE signals were detected from the crack region, with a good location accuracy (Fig. 7). The regions around the bonded tabs also released AE sig-nals, especially at the corners of the aluminium tabs; this was not unexpected since the stress field induced by the loading fixtures is likely to produce a concentration of stresses. Only signals from the crack region were used for this analysis as shown in Fig. 7.

For classification repeatability purposes, only signals recorded by sensor 5 were considered throughout the whole test. Therefore, there are a few signals (as visible in Fig. 7) that were located in the region of interest and were not recorded by sensor 5, although they are a small percentage (around 2% of the total). A sample of the selected waveforms are shown in Fig. 8.

The C-scans at the beginning and after the last batch without impact are shown in Fig. 9. The central sensor (number 5) is always visible in the C-scans as a dark spot with its attached cable running to the left.

C-scans confirm that no additional damage has been introduced during the test. No high attenuation (dark) areas are found; this confirms the absence of in-plane discontinuities, like delaminations. The crack region, below the sensor visible in the centre, appears to darken slightly, but no evidence of growth can be observed.

3.2. Post impact

After the impact, the AE activity of the panel increased significantly. Fig. 10 shows AE localised events for the last batch after impact (batch 31). The test was then interrupted since it showed significant sources from the impact region. The figure also shows the selected events from this set.

The location accuracy appears reduced, mainly due to the presence of the impact area, which alters the wave propagation path, while the original Delta-T calibration was still used. Nevertheless, it can be noticed that signals from the crack area have decreased in number, and moved toward the crack tips. This is a consequence of the crack region having reduced its stiffness: the stress field increases at the sides of the crack, and stress concentration areas are found around the crack tips. Therefore, those signals may indicate some damage mechanisms happening at or near the crack tip regions. A sample of the signals coming from the delamination region is shown in Fig. 11.

The delamination size after impact was determined by C-scanning the panel again, as visible in Fig. 12.

A final C-scan after all fatigue testing was completed indicated that the delamination had not grown significantly (Fig. 12c).

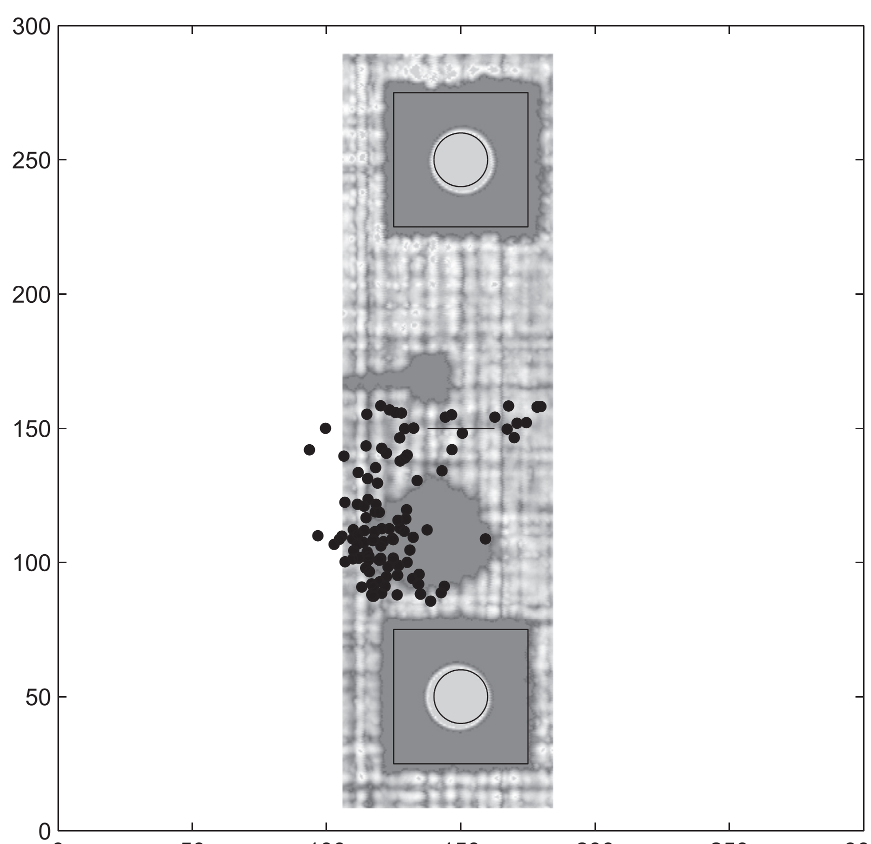

Fig. 13. AE selected events superimposed to the C-scan.

Superimposing AE data to the C-scan, it is clear that only the left border of the impacted area shows AE activity (Fig. 13).

A possible explanation for this, considering that the delamination has not grown, would be that the active areas in the delamination are the ones that experience some type of rubbing or frictional phenomena, in other words those areas that are experiencing a high stress gradient, due to the particular stress field the panel is exposed to.

3.3. Classification of AE signals

Classification of the dataset showed interesting results, with the identification of two classes of signals.

The parameters used for the classification are:

- Amplitude (A), in dB_{AE} (in logarithmic scale, with a reference voltage of 1 mV at the sensor output);

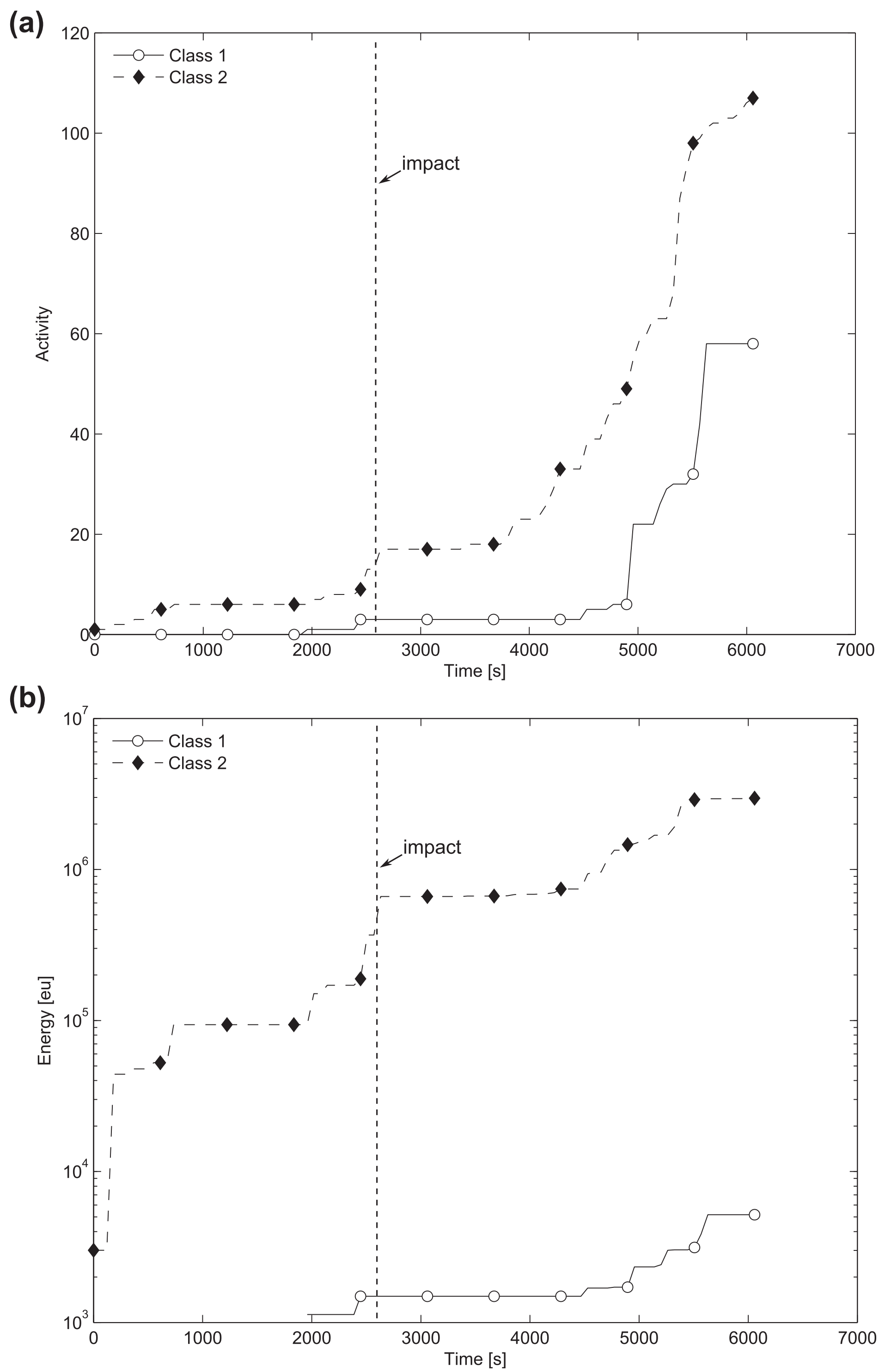

Fig. 14. AE activity (a) and energy (b) trends, after classification.

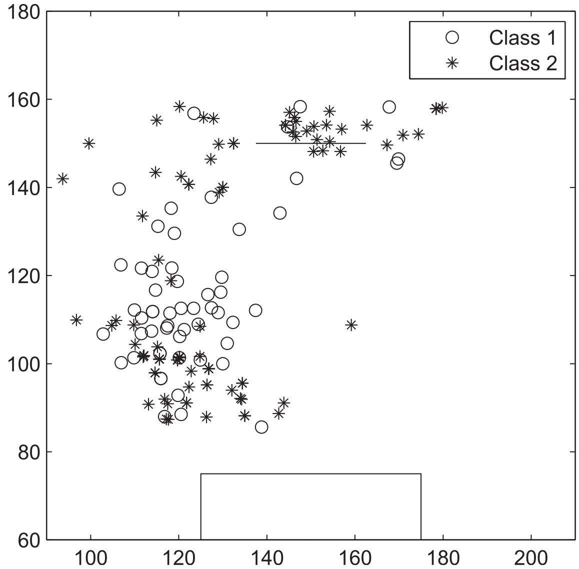

Fig. 15. Classified signals in the selected region.

- Duration (D), in μs;
- Risetime (R), in μs;
- Counts (CNTS), the number of signal zero-crossings;
- Energy (E), in eu (1eu $= 10^{-14}$ V^2s), calculated measuring the area under the signal envelope;
- Frequency center-of-gravity (FCOG), the geometric center frequency of the signal's Fast Fourier Transform (FFT) in kHz;
- Peak Frequency (FMXA), the peak of the signal's FFT in kHz.

The classification technique, presented in detail in Refs. [31], uses a Self-Organizing Map which takes as input the waveform's parameters vector, and gives as output the Best-Matching Unit (BMU). In this way, the SOM maps the multidimensional input to a 2-dimensional space, which is then further mapped to a number of clusters, which themselves correspond to dataset classes. The optimal number of clusters in the dataset is chosen automatically considering a number of classification parameters.

For this dataset, the k-SOM classification technique identified two as the best number of natural classes. AE data has then been classified accordingly.

Global AE energy and activity trends (Fig. 14) show that the first part, before impact (0–2646 s), is dominated by Class 2, while Class 1 remains almost silent. Class 1 is observed at approximately 4500 s, with an increasing trend, which is followed by Class 2.

All classified localised signals for the two batches are shown in detail in Fig. 15.

From this preliminary observation, it can be noted that the crack region holds mainly Class 2 signals, while the impacted area shows a mixture of both classes, with Class 1 being evenly spread and Class 2 concentrating at the bottom boundary.

Energy and activity maps (Fig. 16) show that Class 1 has a lower energy than Class 2, and is concentrated, as previously observed, around the impacted area and at the crack tips. Class 2 is concentrated in the middle of the crack and at the tips, and at the bottom boundary of the impacted area.

Considering the aforementioned time blocks, the evolution of signals is shown in Fig. 17.

Here, the signal evolution indicates that, after impact (Fig. 17b), a number of Class 2 events appear in the damaged region; then, a mixture of Class 1 and Class 2 signals are emitted at a similar rate.

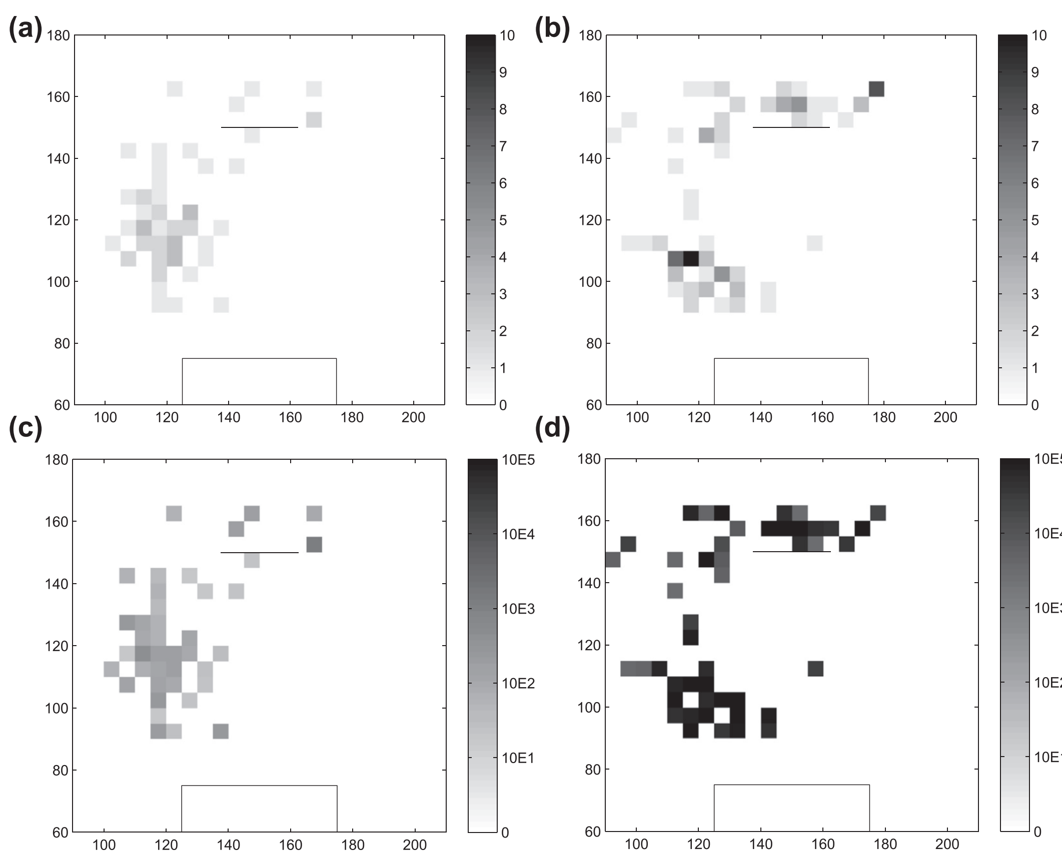

Fig. 16. AE energy and activity 2D maps, by class (a) activity, class 1 (b) activity, class 2 (c) energy, class 1 (d) energy, class 2.

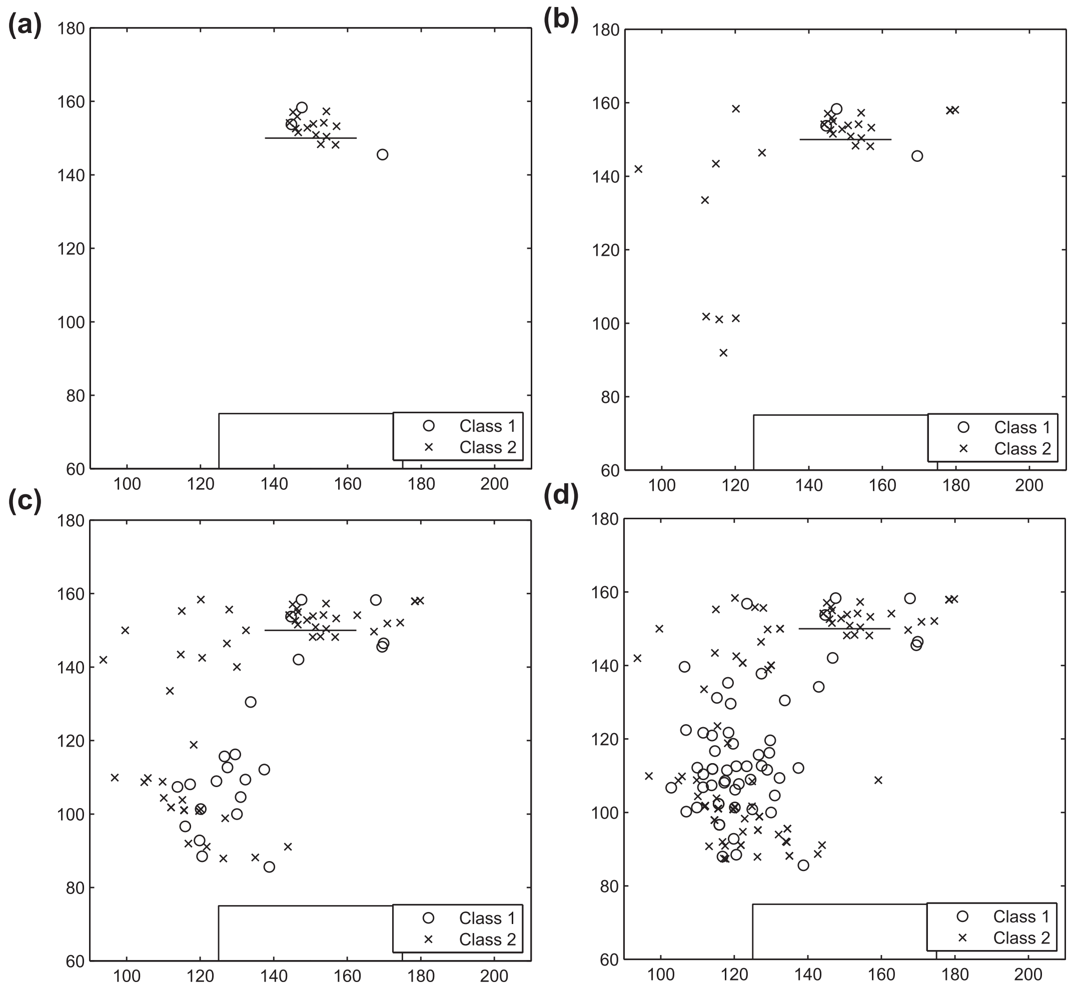

Fig. 17. AE events in time, classified (a) t = 0–2646 s (b) t = 0–4500 s (c) t = 0–5200 s (d) t = 0 to end.

An example of the waveforms from both classes is shown in Fig. 18. Here it is clear that the classification technique is capable of separating two distinct groups of waveform shapes. Also, average parameters for the two classes are reported in Table 3.

4. Discussion

The AE results presented in Section 3 provided some key information and confirmation regarding AE and damage detection in composites:

- Cutting the inner plies allowed the generation of an artificial flaw that favoured matrix cracking;
- The artificial crack area showed repeatable sources, as visible from the waveforms;
- A delamination induced by an impact becomes an active source of AE;
- The delamination source of this experiment contains two distinguishable classes of AE signals;
- The delamination source is active from the AE point of view even if the delamination does not grow.

When supported by ANN classification, the failure modes are correctly identified: the pre-impact phase shows only a single class of signals; when the panel is impacted, a second class appears. It is observed that in the impact region both delamination and crack signals are found.

The crack class signals seem to be more related to the region normal to the load path (matrix failing in tensile load); this is supported by the AE signals position relative to the delamination area observed in the C-scan and by the observation of almost only crack class signals in the cut ply region.

On the other hand, the delamination class signals are distributed in the delamination region, probably originated by debonded layer friction. Although this does not imply delamination growth, it provides a way to identify the delamination region, which may cause a significant reduction in structural compressive strength of the component.

It was also observed that the two classes show repeatable sources, with distinct waveforms and AE parameters. In particular, matrix cracking sources show higher amplitude and a relatively quicker decay, while delamination sources appear as a continuous-like source.

The augmentation of AE data with automatic classification information presented in this work represents an improvement for the use of AE as SHM system for carbon components. If a component is fitted with an AE sensor network and its signals are classified according to the procedure presented, the human discretion in interpreting AE trends and signals is significantly reduced, if not completely removed, when deciding if a component has developed a new damage mode.

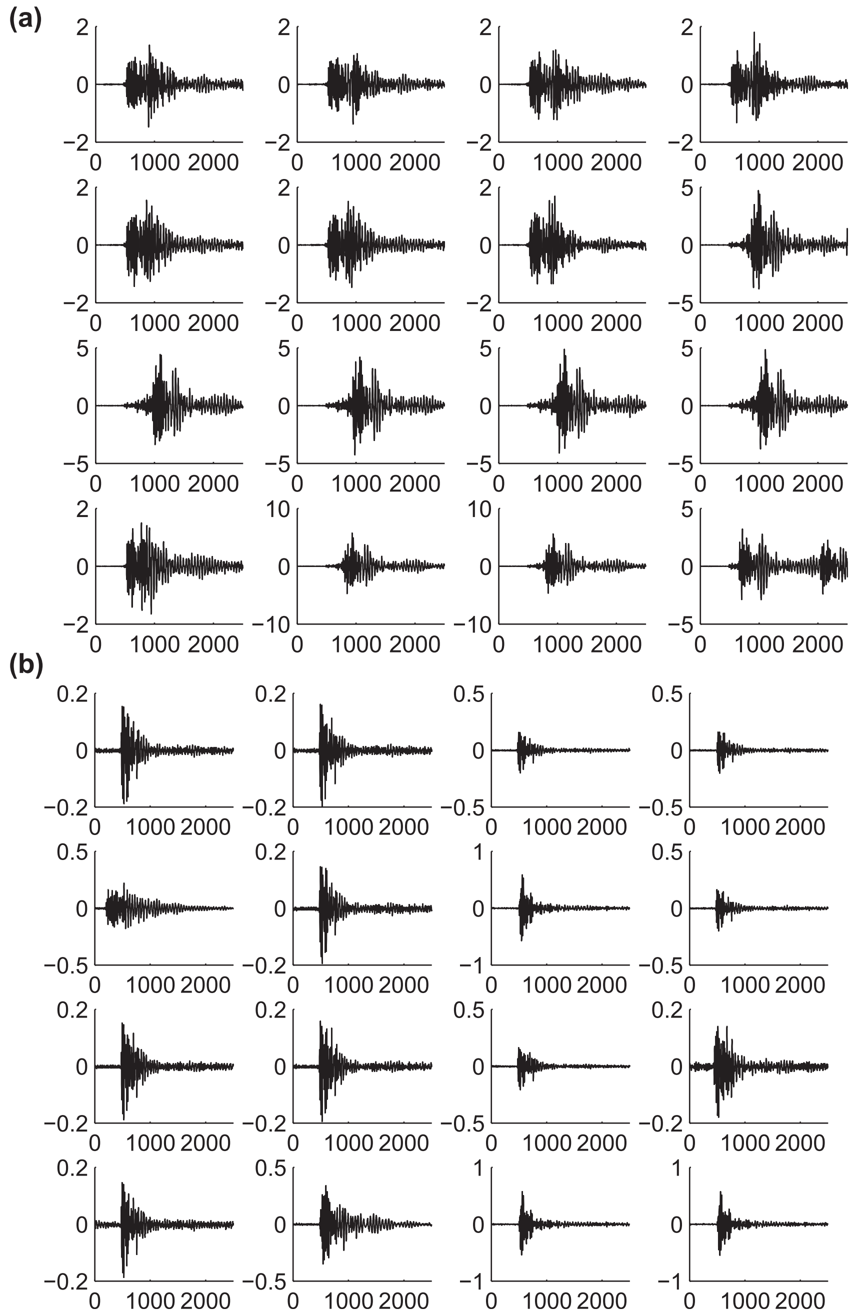

Fig. 18. Waveforms from class 1 (a) and class 2 (b).

An important feature to stress is, that if AE data is presented without classification data, it is not possible to discriminate whether a change in activity is related to a particular damage mode developing, or whether it is only a change in environmental conditions (e.g. noise). By coupling AE location data and classification information, it would be possible to separate the various contributions of the different classes, and monitor them separately both by location and in their time evolution.

This feature will be a benefit for real-time monitoring, maintenance and also laboratory component testing, since the use of AE may give precious indications to the system operator about damage characteristics, location and evolution, without involving direct human intervention or downtime for inspection. In the design phase of parts intended to be monitored, SHM will help limit both the weight

Table 3
Average parameters for the two classes.

	Class 1		Class 2	
	Average	Std. deviation	Average	Std. deviation
CNTS	3	4	85	41
A (dB)	49	3	69	6
E (eu)	89	151	27,680	28,732
R (μs)	8	20	94	126
D (μs)	25	33	810	504
FCOG (kHz)	263	38	266	59
FMXA (kHz)	224	57	174	77

of the structure and the involved safety factors. A SHM technique which provides precise information on each damage mode evolution reduces the uncertainties of the damage models themselves and consequently decrease inspection intervals. SHM alarms can therefore trigger direct, localized and focussed maintenance.

5. Conclusions

This experimental work presented a way of generating two distinct artificial AE signal sources in a CFRP plate, one related to matrix cracking phenomena and a second one related to impact-induced in-plane delamination. A neural network-based fully automated classification technique proved to be effective in identifying these two different sources and to correctly separate them. This was supported by visual observation and ultrasonic C-scanning.

The AE technique, supported both by advanced location algorithms (namely the Delta-T technique) and automatic classification methods (the k-SOM classifier), proved to be valid to monitor in real-time CFRP structures under fatigue load, and could be easily made capable of automatically identifying the onset of a novel damage mode in real-time.

Criteria for rejection or acceptance of parts (i.e. defining alarm levels and assessing false alarm probabilities) have yet to be investigated deeply. Also, the applicability of the classification technique to real-time AE data classification without having to consider the entire dataset is being evaluated at the moment.

Acknowledgements

The authors would like to acknowledge the support of Cardiff University – School of Engineering laboratories, facilities and staff for the support given during the experimental part of this work.

References

[1] Worden K, Farrar CR, Manson G, Park G. The fundamental axioms of structural health monitoring. Proc R Soc A Math Phys Eng Sci 2007;463:1639–64.
[2] Miller RK, McIntire P. NDT handbook, vol. 5. American Society for Nondestructive Testing; 1987. p. 652.
[3] Finlayson RD. Acoustic emission testing. In: Hellier C, editor. Handbook of nondestructive evaluation. McGraw-Hill Companies; 2003. 10.1–10.39.
[4] Huang M, Jiang L, Liaw PK, Brooks CR, Seeley R, Klarstrom DL. Using acoustic emission in fatigue and fracture materials research. J Oncol Manag 1998:50.
[5] Hamstad MA. Thirty years of advances and some remaining challenges in the application of acoustic emission to composite materials. In: Kishi T, Ohtsu M, Yuyama S, editors. Acoust. emiss. beyond Millenn. Oxford, UK: Elsevier; 2000. p. 77–91.
[6] Wang X, Zhang H-P, Yan X. Classification and identification of damage mechanisms in polyethylene self-reinforced laminates by acoustic emission technique. Polym Compos 2011;32:945–59.
[7] Caruso C, Lonetti P, Manna A. Dynamic crack propagation in fiber reinforced composites. In: Proc. COMSOL conf. 2009 Milan; 2009.
[8] Jessen SM, Plumtree A. Fatigue damage accumulation in pultruded glass/polyester rods. Composites 1999;20:559–67.
[9] Bourchak M, Farrow I, Bond I, Rowland C, Menan F. Acoustic emission energy as a fatigue damage parameter for CFRP composites. Int J Fatigue 2007;29(3):457–70.
[10] Ireman T, Ranvik T, Eriksson I. On damage development in mechanically fastened composite laminates. Compos Struct 2000;49:151–71.
[11] Caprino G, Teti R, de Iorio I. Predicting residual strength of pre-fatigued glass fibre-reinforced plastic laminates through acoustic emission monitoring. Compos Part B 2005;36:365–71.
[12] Baxter MG, Pullin R, Holford KM, Evans SL. Delta T source location for acoustic emission. Mech Syst Signal Process 2007;21:1512–20.
[13] Eaton MJ, Pullin R, Holford KM. Acoustic emission source location in composite materials using Delta T mapping. Compos Part A Appl Sci Manuf 2012;43:856–63.
[14] HSU NN. A mechanical AE simulator for system calibration and waveform analysis. In: 16th Meet. U.S. Acoust. Emiss. Work. Gr., Williamsburg, Va, United States; 1976.
[15] Holford KM, Pullin R, Baxter MG. Modal analysis of acoustic emission signals from artificial and fatigue crack sources in aerospace grade steel. Key Eng Mater 2005;293:217–24.
[16] Mal A. Elastic waves from localized sources in composite laminates. Int J Solids Struct 2002;39:5481–94.
[17] Huguet S, Godin N, Gaertner R, Salmon L, Villard D. Use of acoustic emission to identify damage modes in glass fibre reinforced polyester. Compos Sci Technol 2002;62:1433–44.
[18] Zhuang X, Yan X. Investigation of damage mechanisms in self-reinforced polyethylene composites by acoustic emission. Compos Sci Technol 2006;66:444–9.
[19] Ramirez-Jimenez CR, Papadakis N, Reynolds N, Gan TH, Purnell P, Pharaoh M. Identification of failure modes in glass/polypropylene composites by means of the primary frequency content of the acoustic emission event. Compos Sci Technol 2004;64:1819–27.
[20] Groot PJ De, Wijnen PAM, Janssen RBF. Real-time frequency determination of acoustic emission for different fracture mechanisms in carbon/epoxy composites. Compos Sci Technol 1995;55:405–12.
[21] Godin N, Gaertner SHR, Salmon L. Clustering of acoustic emission signals collected during tensile tests on unidirectional glass/polyester composite using supervised and unsupervised classifiers. NDT E Int 2004;37:253–64.
[22] Refahi Oskouei A, Ahmadi M. Acoustic emission characteristics of Mode I delamination in glass/polyester composites. J Compos Mater 2010;44:793–807.
[23] Laksimi A, Benmedakhene S, Bounouas L. Monitoring acoustic emission during tensile loading of thermoplastic composites materials. In: Proc. ICCM 12 Eur; 1999.
[24] Godin N, Huguet S, Gaertner R. Influence of hydrolytic ageing on the acoustic emission signatures of damage mechanisms occurring during tensile tests on a polyester composite: application of a Kohonen's map. Compos Struct 2006;72:79–85.
[25] Grosse C, Reinhardt H, Dahm T. Localization and classification of fracture types in concrete with quantitative acoustic emission measurement techniques. NDT E Int 1997;30:223–30.
[26] Leone C, Caprino G, de Iorio I. Interpreting acoustic emission signals by artificial neural networks to predict the residual strength of pre-fatigued GFRP laminates. Compos Sci Technol 2006;66:233–9.
[27] De Oliveira R, Marques AT. Health monitoring of FRP using acoustic emission and artificial neural networks. Comput Struct 2008;86:367–73.
[28] Bhat C, Bhat MR, Murthy CRL. Acoustic emission characterization of failure modes in composites with ANN. Compos Struct 2003;61:213–20.
[29] Doan DD, Ramasso E, Placet V, Boubakar L, Zerhouni N. An unsupervised pattern recognition approach for AE data originating from fatigue tests on polymer-composite materials. In: Proc EWSHM-7th European workshop on SHM Nantes, France; 2014.
[30] Sause MGR, Gribov A, Unwin AR, Horn S. Pattern recognition approach to identify natural clusters of acoustic emission signals. Pattern Recognit Lett 2012;33:17–23.
[31] Crivelli D, Guagliano M, Monici A. Development of an artificial neural network processing technique for the analysis of damage evolution in pultruded composites with acoustic emission. Compos Part B 2014;56:948–59.